Topological Reconstruction of a Smooth Manifold-Solid From Its Occluding Contour

Lance R. Williams

CMPSCI TR94-04

February1994

This work was supported by the Advanced Research Projects Agency (via TACOM) under contract number DAAE07-91-C-RO35, and by the National Science Foundation under grant number CDA-8922572.

Topological Reconstruction of a Smooth Manifold-Solid from its Occluding Contour

Lance R. Williams
NEC Research Institute
4 Independence Way
Princeton, NJ 08540
williams@research.nj.nec.com

Abstract

This paper describes a simple construction for building a combinatorial model of a smooth manifold-solid from a labeled figure representing its occluding contour. The motivation is twofold. First, deriving the combinatorial model is an essential intermediate step in the visual reconstruction of solid-shape from image contours. A description of solid-shape consists of a metric and a topological component. Both are necessary: the metric component specifies how the topological component is embedded in three-dimensional space. The *paneling construction* described in this paper is a procedure for generating the topological component from a labeled figure representing the occluding contour. Second, the existence of this construction establishes the sufficiency of a labeling scheme for line-drawings of smooth solid-objects originally proposed by Huffman[6]. By sufficiency, it is meant that every set of closed plane-curves satisfying this labeling scheme is shown to correspond to a generic view of a manifold-solid. Together with the Whitney theorem[17], this confirms that Huffman's labeling scheme correctly distinguishes possible from impossible solid-objects.

1 Introduction

The larger problem which initiated the research described in this paper is the reconstruction of solid-shape from image contours, a topic at the heart of computer vision. Broadly speaking, it is proposed that the Huffman labeling scheme for smooth solid-objects[6] can function as a two-dimensional intermediate representation, bridging the gap between image contours and three-dimensional solid-objects. While Huffman's influential paper "Impossible Objects as Nonsense Sentences" is widely cited as one source of the Huffman-Clowes junction catalog for trihedral scenes, the last few pages of Huffman's paper is devoted to a labeling scheme for smooth objects (see Figure 1). Huffman's labeling scheme differs from the labeling scheme proposed by Malik[10] in two important ways. First, Malik assumes *piecewise smooth surfaces without boundary*, while Huffman assumes *smooth surfaces with and without boundary.* Although these domains overlap, they are distinct. Second, like other contour labeling work in computer vision (e.g. [3, 16, 7]), Malik considers only visible contours, while Huffman explicitly considers both visible and *occluded* contours.

A smooth surface embedded in three-space generates a set of image contours which can be classified as either: 1) the image of boundaries; or 2) occluding contours. Boundaries are the image of points with neighborhoods topologically equivalent to half-discs (i.e. like the edge of a sheet of paper). Occluding contours are the image of points where the surface is tangent to the viewing direction (i.e. the image of the *contour generator*). Because the surface which forms the boundary of a smooth manifold-solid is closed, its image will contain no boundaries—only occluding contours. Therefore, in this paper, we only consider a subset of the Huffman labeling scheme (i.e. (c) through (f) in Figure 1).

A solid-shape description contains two components. The first is topological, and specifies a set of neighborhoods (i.e. a topology). The second component describes how those neighborhoods are embedded in three-dimensional space. The neighborhoods of the surface which forms the boundary of a manifold-solid can be explicitly represented by means of a combinatorial model called a *paneling.* The term "paneling" is used by Griffiths[4] in his informal but very accessible account of the topology of surfaces. Roughly speaking, a paneling is a set of paper *panels* taped together in prescribed ways. The paneling is produced by applying a straightforward procedure called the *paneling construction* to a labeled figure representing the occluding contours comprising the image of a smooth manifold-solid.

1.1 Solid-Shape from Image Contours

It is proposed that a description of solid-shape can be computed from image contours (or a line-drawing) by means of the three-stage process depicted in Figure 2(a). The first stage is *figural completion*, which is the process of inferring a set of interpolating curves, or *completions*, satisfying the Huffman labeling scheme. A non-trivial example of a figural completion problem in the domain of smooth manifold-solids is shown in Figure 3. In his recent Ph.D. thesis[19], the author describes a working system which solves figural completion problems in the *anterior scene* domain (see Figure 4). An anterior scene is a set of smooth surfaces with boundary embedded in three-dimensional space such that the surface normals everywhere have a positive component in the viewing direction. These results, while preliminary, suggest that similiar methods may succeed in the more complex domain of smooth manifold-solids.

The second stage in the reconstruction of a smooth manifold-solid from image contours is the topic of this paper—the paneling construction. The paneling construction translates the

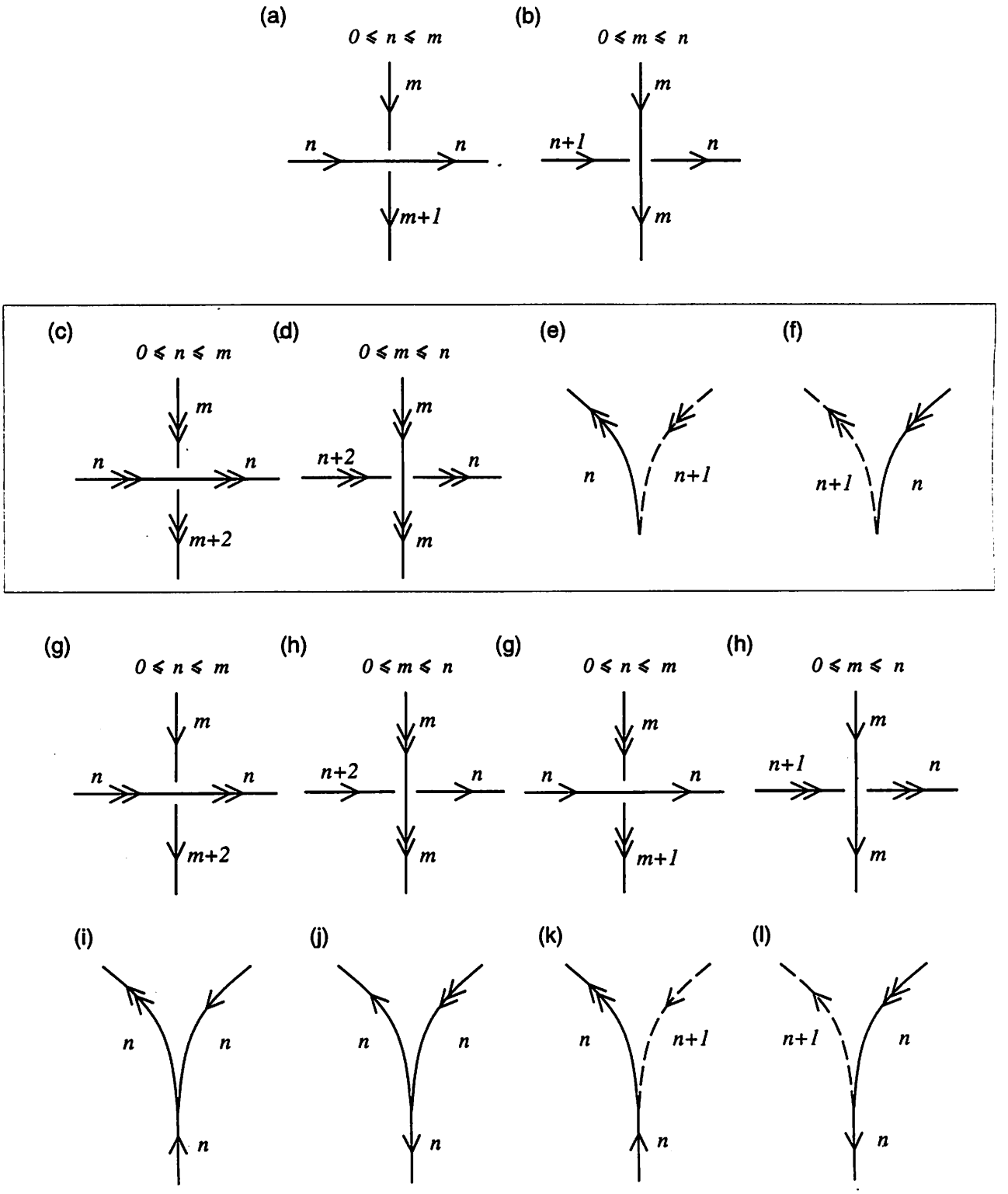

Figure 1: Huffman's labeling scheme for smooth objects. Numbers are depth indices and arrows indicate sign of occlusion. (a) and (b) Boundary crossing junctions are sufficient to represent the domain of *anterior scenes*[19]. An anterior scene is a set of smooth surfaces with boundary embedded in three-dimensional space such that the surface normals everywhere have a positive component in the viewing direction. (c) through (f) Occluding contour crossing junctions and cusp junctions together define the domain of *smooth manifold-solids*. (g) through (l) Additional junction types required for arbitrary smooth objects.

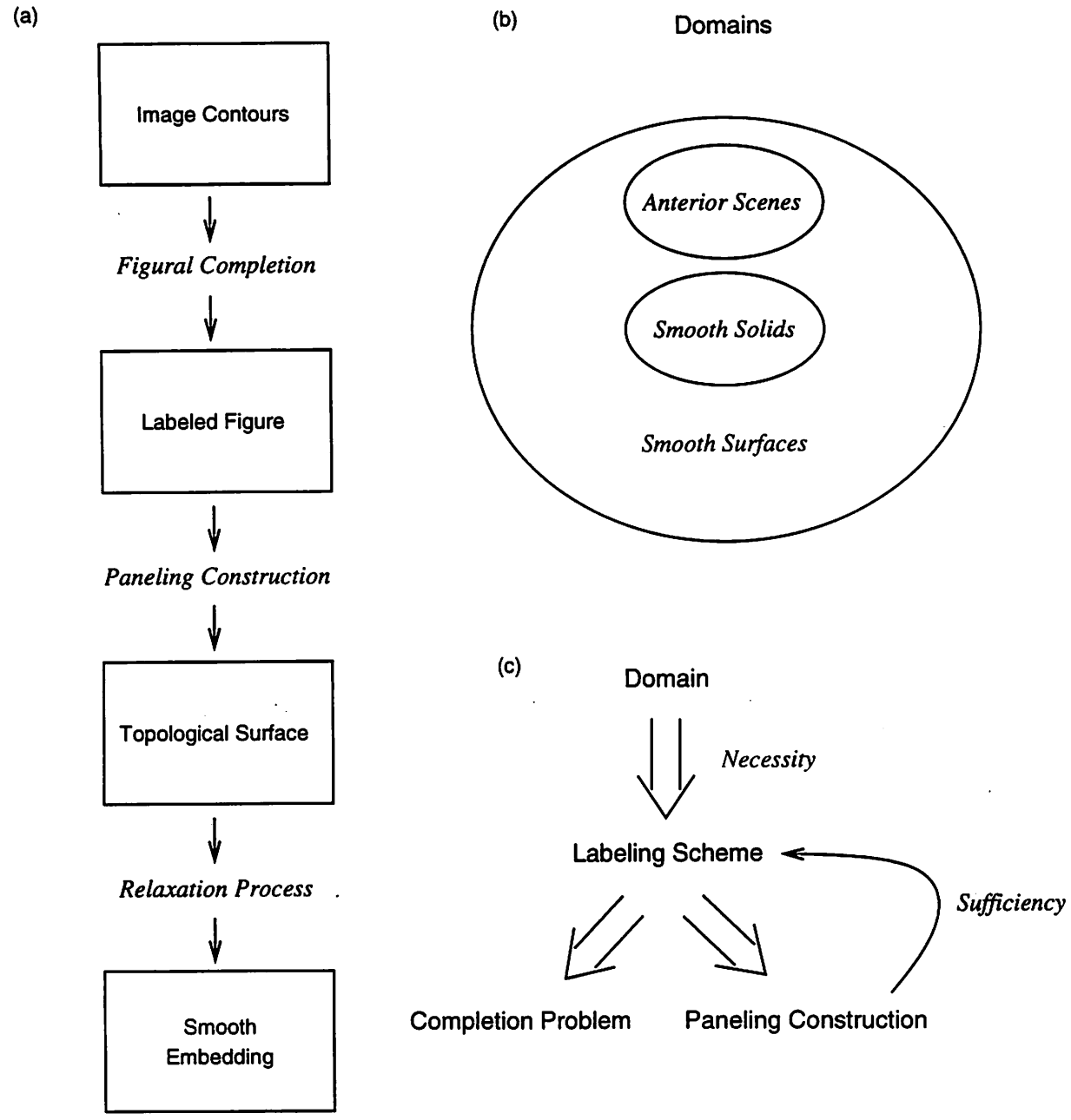

Figure 2: (a) A strategy for reconstructing smooth objects from image contours. (b) Venn diagram showing relationship of problem domains. (c) For any given problem domain, necessary constraints on depth indices and sign of occlusion define a contour labeling scheme. For each labeling scheme, there is an associated *completion problem* and a *paneling construction.* Both are intermediate steps in the process of reconstructing a smooth object from image contours. Finally, the existence of a paneling construction for a given labeling scheme establishes its *sufficiency* as a representation and as a source of grouping constraints.

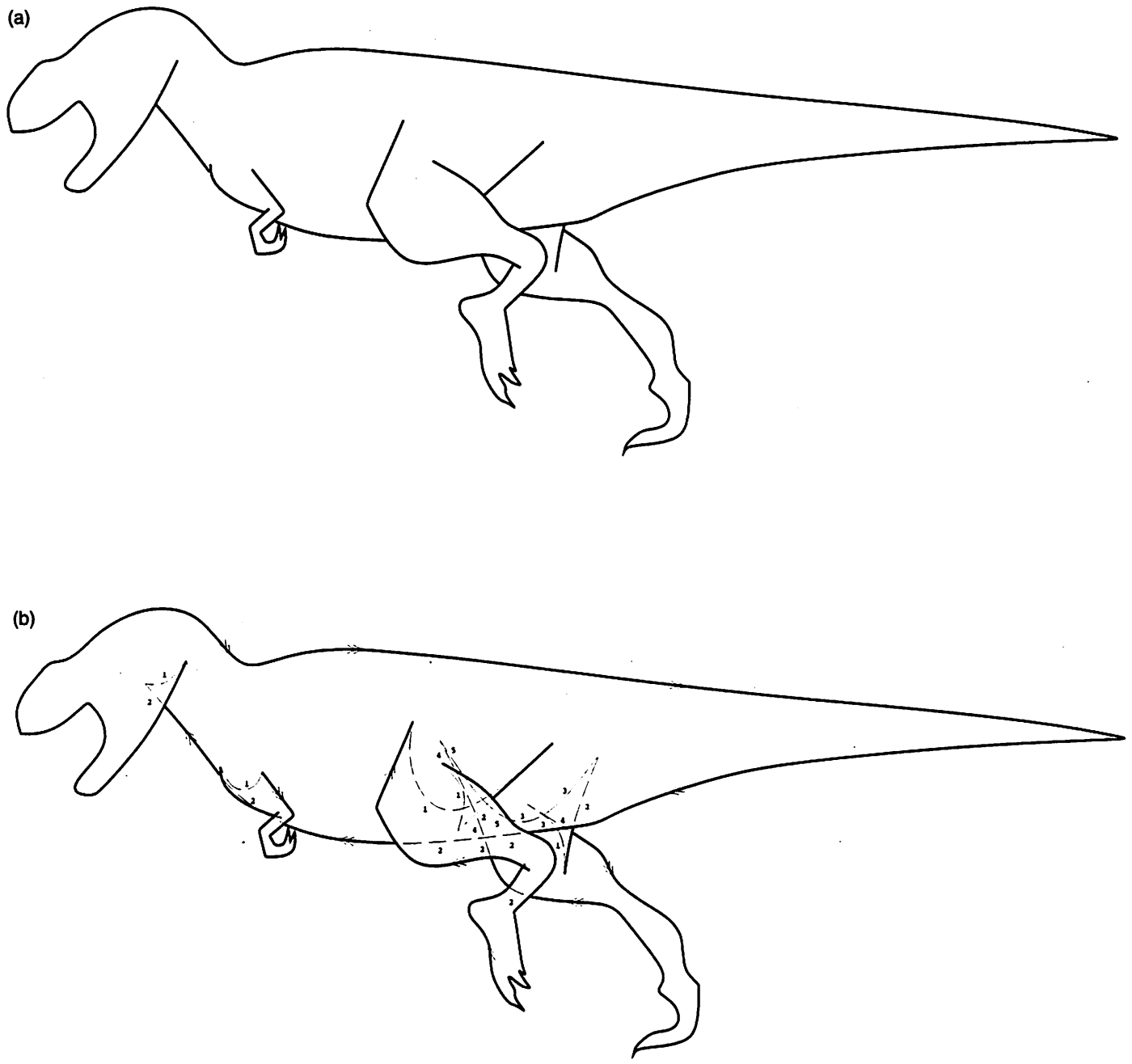

Figure 3: Figural completion problem for smooth manifold-solid. (a) Visible occluding contours for *Tyrannosaurus rex* solid [Note: Adapted from figure by Gregory S. Paul[11]]. (b) Completed and labeled occluding contours for *Tyrannosaurus rex* solid. Figural completion is the problem of computing (b) given (a). It is proposed that sets of closed plane curves satisfying the Huffman labeling scheme can function as a two-dimensional intermediate representation, bridging the gap between image contours and three-dimensional solid-objects.

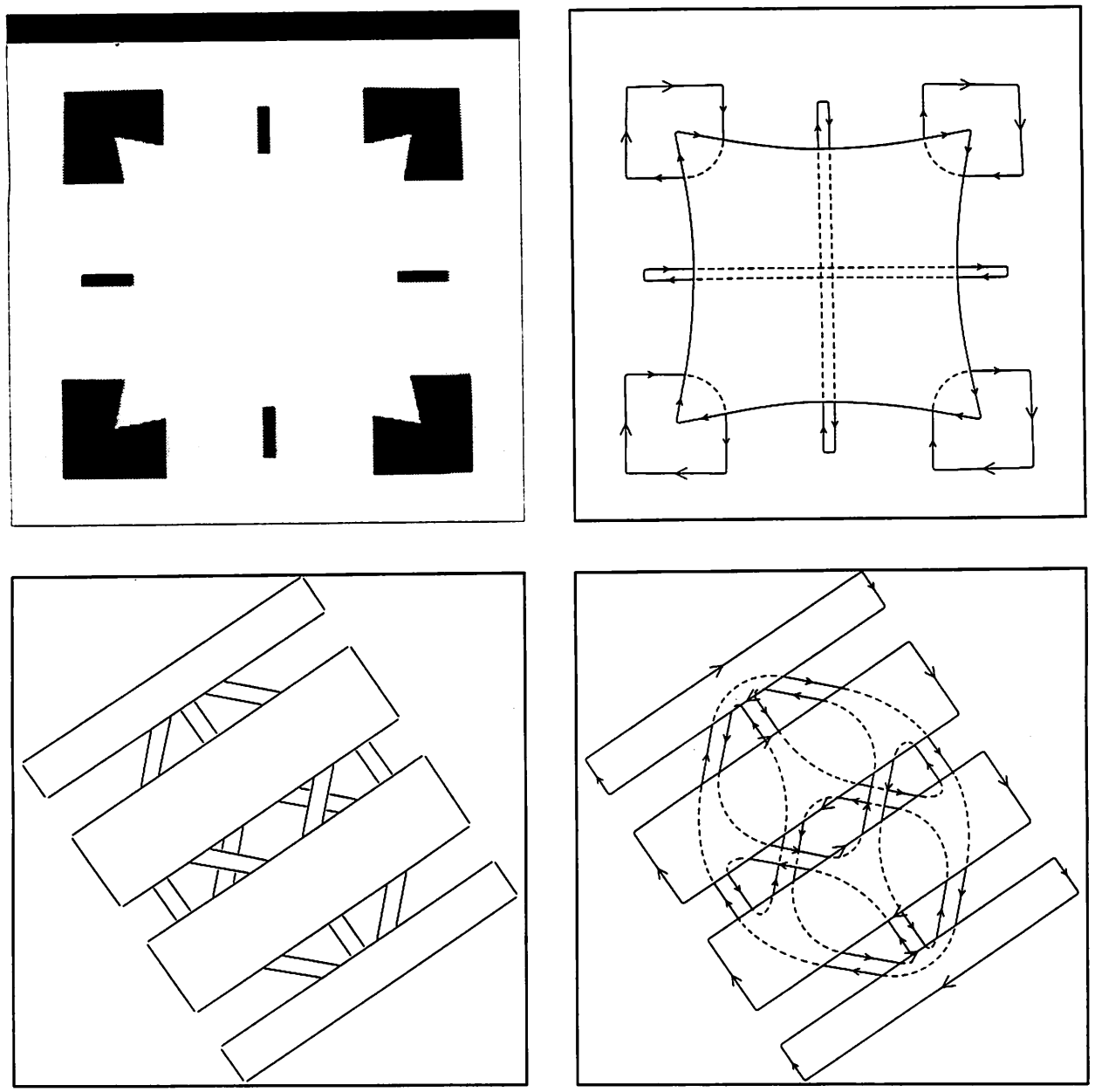

Figure 4: In his recent Ph.D. thesis [19] the author describes a working system which solves figural completion problems in the *anterior scene* domain. The upper left figure is a typical illusory contour stimulus. The output of the experimental implementation is shown in upper right. The lower left figure is a modified version of a figure designed by Kanizsa[8]. The output of the experimental implementation is shown in lower right. Interpolations are smooth due to the use of minimum energy cubic Bezier splines to represent completion shapes. These results, while preliminary, suggest that similiar methods may succeed in the more complex domain of smooth manifold-solids.

labeled figure (which is the product of the figural completion process) into a combinatorial model of an orientable surface without boundary. Stated differently, it makes explicit the topology of the solid-shape implicit in the labeled figure. This is a prerequisite for the final stage, the goal of which is to compute a smooth embedding of the paneling in three-dimensional space.

Recent work by Szeliski, Tonnesen and Terzopolous[14] also addresses the issue of topological reconstruction. The paneling construction described in this paper complements their work by considering the case where the input is an occluding contour. Indeed, oriented particle systems might be the best way to implement the paneling construction in actual practice.

Richards, Koenderink and Hoffman[12] discuss an entirely different completion problem relevant to the embedding of the paneling in space—the problem of inferring the complete trace of the *parabolic lines* on the surface of a smooth manifold-solid. The completed parabolic lines must connect inflection points in the silhouette without crossing on the surface. Because the parabolic lines demarcate regions of positive and negative Gaussian curvature, they are an important aspect of solid-shape. However, Richards *et al.* consider only the genus zero case and assume that the occluding contour contains no crossings or cusps, so that the topology of the surface is fixed. They do not address the issue of topological reconstruction of the surface, but it would seem that this must logically preceed completion of the parabolic lines.

Terzopolous, Kass and Witkin[15] have experimentally demonstrated reconstruction of simple solid-shapes from silhouettes under assumptions similiar to those described above. Basically, they assume that the topology of the object can be described by a tube centered on a user-specified medial-axis. The embedding of the tube in space minimizes an energy functional which combines membrane and thin-plate terms with terms derived from image brightness. It is reasonable to suppose that a method similiar to that of Terzopolous *et al.* could be used to find a smooth embedding of a paneling produced by the construction proposed in this paper.

1.2 Possible and Impossible Smooth Solid-Objects

The other source of motivation for this work is theoretical. The existence of the paneling construction establishes the sufficiency of Huffman's labeling scheme for line-drawings of smooth solid-objects. By sufficiency, it is meant that every set of closed plane-curves satisfying this labeling scheme is shown to correspond to a *generic view* of a smooth manifold-solid. If the view of the manifold-solid is generic, then the crossings will be the only points of multiplicity two in the projection of the contour generator onto the plane:

Defn. *generic view - an image of a smooth manifold-solid where: 1) the multiplicity of the image of the contour generator is one everywhere except at a finite number of points where it is two; and 2) the number of multiplicity two points is invariant to small changes in viewing direction.*

In an influential paper, Koenderink and van Doorn[9] describe the singularities of the visual mapping of a smooth manifold-solid onto the image plane under parallel projection. Largely through this paper, researchers in computer vision have become aware of a theorem due to Whitney which holds that the only generic singularities of mappings of smooth surfaces onto the plane are *folds* and *cusps* (see [17, 1]).

Let $\mathcal{F}$ be the space of figures satisfying the Huffman labeling scheme for smooth solid-objects and let $\mathcal{G}$ be the space of generic views of smooth manifold-solids. Then the Whitney theorem tells us that $\mathcal{G} \subseteq \mathcal{F}$, that is, there are no generic views of smooth manifold-solids that do not have corresponding labeled figures. In this paper, the converse, $\mathcal{F} \subseteq \mathcal{G}$, is proven. Stated differently, the existence of the paneling construction shows that every labeled figure corresponds to a generic view of a manifold-solid. Together, this confirms that the labeling scheme consisting of (c) through (f) in Figure 1 correctly distinguishes possible from impossible smooth solid-objects (i.e. $\mathcal{G} \equiv \mathcal{F}$).

2 Sufficiency of Labeling Scheme

We now show that every set of closed plane-curves satisfying the labeling scheme illustrated in Figure 5 represents a generic view of a manifold-solid. First, constraints on the number of surface points which project to a single image point are identified. We then demonstrate that given a labeled figure, values satisfying these constraints can always be found. This is a precondition for the paneling construction, which is then described. Finally, we show that every paneling constructed by this procedure represents a manifold-solid which projects generically as the labeled figure.

Theorem *Every set of closed plane curves satisfying the labeling scheme illustrated below represents a generic view of a manifold-solid.*

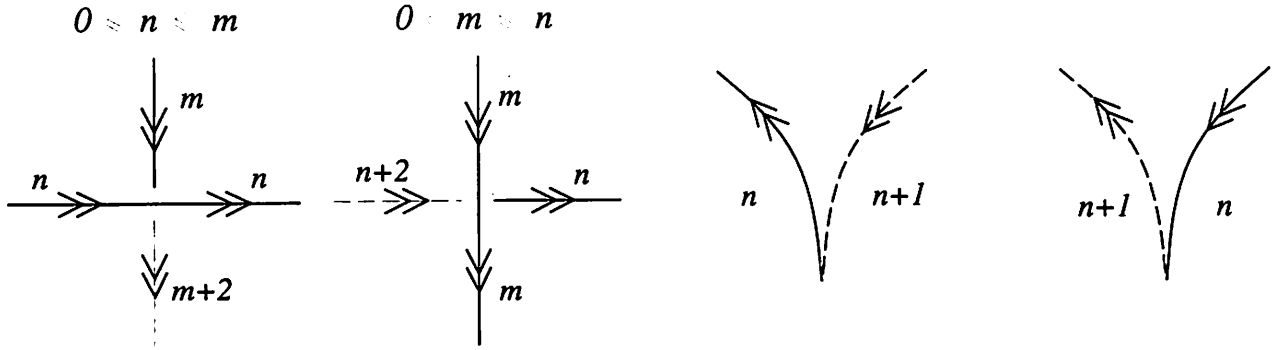

Figure 5: Huffman labeling scheme for smooth solid-objects.

Proof Observe that a set of closed-plane curves partitions the plane into regions. The boundary of each planar region is a cycle of oriented edges separated by crossings and cusps. Every edge forms the side of exactly two planar regions, one lying to its right, the other to its left (where right and left are with respect to the edge's orientation). Note that if an edge is the projection of an occluding contour, then the multiplicity of the projection of interior surface points onto image points is two greater on the right side of the edge than on the left. Furthermore, the multiplicity of the projection of interior surface points onto image points will be constant within a planar region.

Let A and B be neighboring regions and let A lie to the right of B. If the labeled figures represents a manifold-solid, and if γ_A and γ_B are the multiplicities of the projection of interior surface points within regions A and B, then $\gamma_A - \gamma_B = 2$. Observe that the set

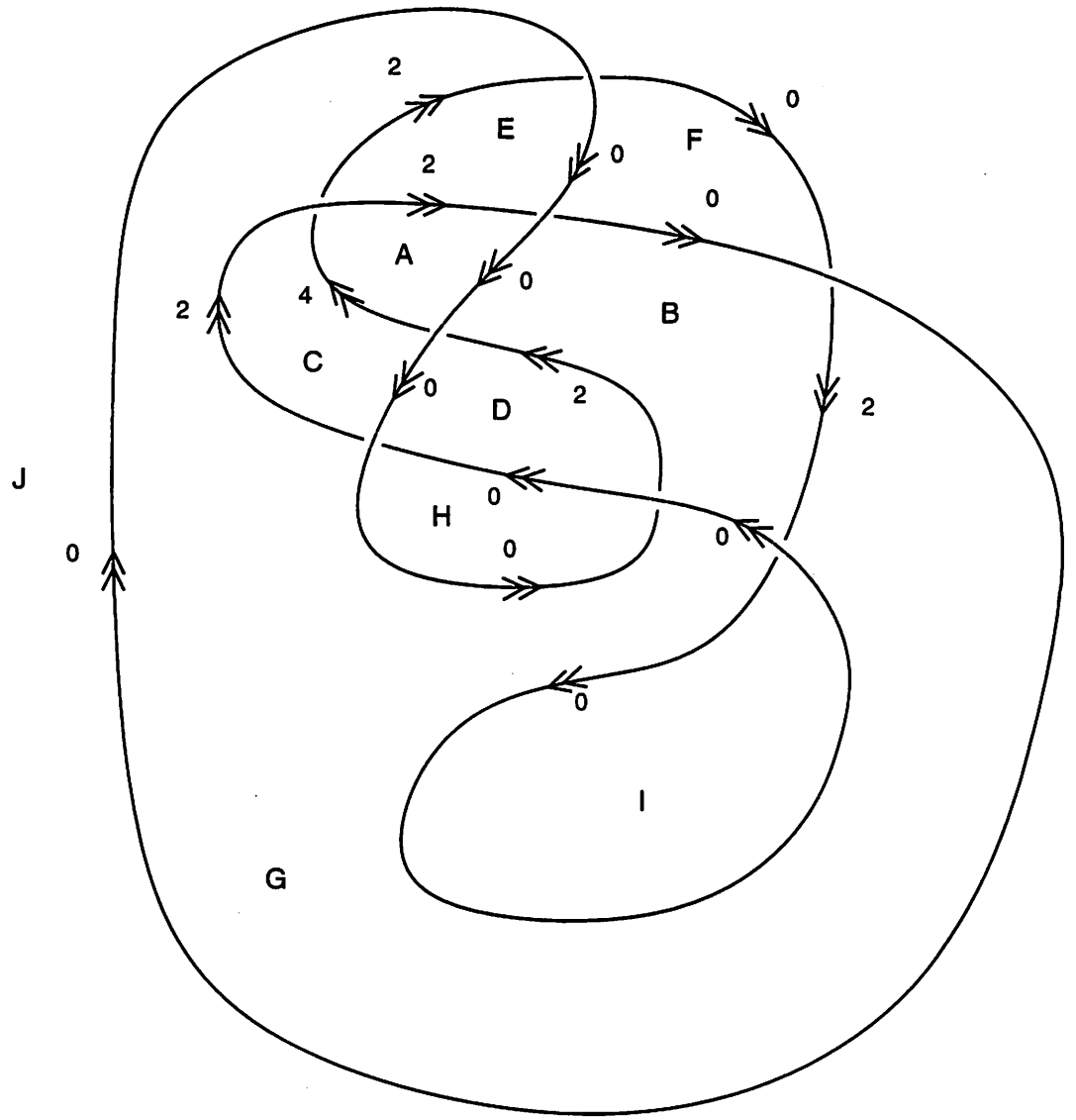

Figure 6: A set of closed plane-curves satisfying the labeling scheme partitions the plane into regions.

of difference constraints among all neighboring planar regions form the node-edge incidence matrix of a network. Let the nodes of the network corresponding to A and B be v_A and v_B respectively. We adopt the convention that the edge of the network joining v_A with v_B is directed from v_A to v_B when region A lies to the right of region B so that the weight of an edge in the network is equal to two when traversed in the direction of its orientation and minus two when traversed in the opposite direction.

Example

Figure 7 illustrates a network constructed in this fashion for the planar partition depicted in Figure 6. The linear system of difference equations represented by this network appear below:

$$\begin{bmatrix} 1 & -1 & 0 & 0 & 0 & 0 & 0 & 0 & 0 & 0 \\ 1 & 0 & -1 & 0 & 0 & 0 & 0 & 0 & 0 & 0 \\ 1 & 0 & 0 & 0 & -1 & 0 & 0 & 0 & 0 & 0 \\ 0 & 1 & 0 & -1 & 0 & 0 & 0 & 0 & 0 & 0 \\ 0 & 1 & 0 & 0 & 0 & -1 & 0 & 0 & 0 & 0 \\ 0 & 1 & 0 & 0 & 0 & 0 & -1 & 0 & 0 & 0 \\ 0 & 0 & 1 & -1 & 0 & 0 & 0 & 0 & 0 & 0 \\ 0 & 0 & 1 & 0 & 0 & 0 & -1 & 0 & 0 & 0 \\ 0 & 0 & 0 & 1 & 0 & 0 & 0 & -1 & 0 & 0 \\ 0 & 0 & 0 & 0 & 1 & -1 & 0 & 0 & 0 & 0 \\ 0 & 0 & 0 & 0 & 1 & 0 & -1 & 0 & 0 & 0 \\ 0 & 0 & 0 & 0 & 0 & 1 & 0 & 0 & 0 & -1 \\ 0 & 0 & 0 & 0 & 0 & 0 & 1 & -1 & 0 & 0 \\ 0 & 0 & 0 & 0 & 0 & 0 & 1 & 0 & -1 & 0 \\ 0 & 0 & 0 & 0 & 0 & 0 & 1 & 0 & 0 & -1 \end{bmatrix} \begin{bmatrix} \gamma_A \\ \gamma_B \\ \gamma_C \\ \gamma_D \\ \gamma_E \\ \gamma_F \\ \gamma_G \\ \gamma_H \\ \gamma_I \\ \gamma_J \end{bmatrix} = \begin{bmatrix} 2 \\ 2 \\ 2 \\ 2 \\ 2 \\ 2 \\ 2 \\ 2 \\ 2 \\ 2 \\ 2 \\ 2 \\ 2 \\ 2 \\ 2 \end{bmatrix}$$

Recall that a system of difference equations has a solution if and only if the sums of the weights of every cycle in its corresponding network equal zero (where the weight of an edge is k or $-k$ depending on the direction of traversal). We demonstrate not only that a solution to this system of difference constraints always exists but also that a solution exists where the value of γ for every planar region is greater than the largest depth index among all edges bordering that region in the labeled figure. Fortunately, this second condition is easy to satisfy, since it is always the case that if $\{x_1, x_2, ..., x_n\}$ is a solution to a system of difference equations, then $\{x_1 + c, x_2 + c, ..., x_n + c\}$ is also a solution for any constant c (and there are no other solutions). Since a sufficiently large c can always be found[1] it is sufficient to prove that the sums of the weights around every closed cycle in a network constructed as described equal zero.

We begin by proving the following lemma:

Lemma *Let J be an oriented Jordan curve in the plane and let C be an arbitrary, oriented, closed plane-curve. If J intersects C at m points, and if $\vec{j}_i$ and $\vec{c}_i$ are the vectors tangent to J and C at these points, then $\sum_{i=0}^{m-1} \mathrm{sgn}(\vec{j}_i \times \vec{c}_i) = 0$.*

Proof A Jordan curve divides the plane into two disjoint regions which we call the *black region* and the *white region.* We adopt the convention that the black region lies to the right as the Jordan curve is traversed in the direction of its orientation while the white region lies

[1] Clearly, the simplest solution will use the smallest possible value of c.

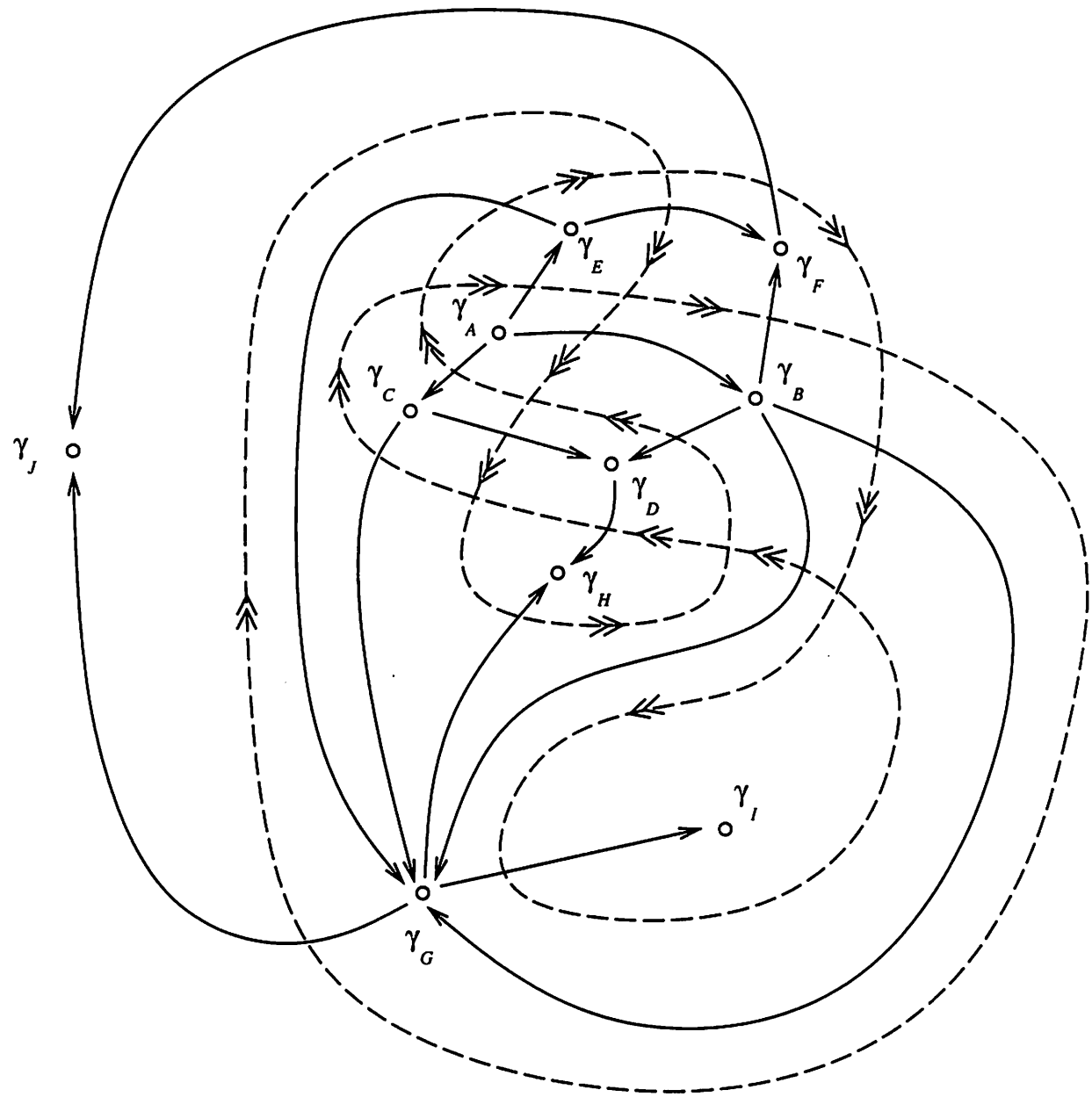

Figure 7: Multiplicity network. A network representing difference constraints on the multiplicity of the projection of interior surface points onto adjacent planar regions. The weights of edges in the network are 2 when traversed in the direction of the arrows and -2 when traversed in the opposite direction. The labeled closed plane-curve from the previous figure is shown dotted.

to the left. If in the course of traversing oriented plane curve C, an ant crosses Jordan curve J at crossing i, then the ant is conveyed either from the black region to the white region or from the white region to the black region. In the first case, $\text{sgn}(\vec{j}_i \times \vec{c}_i) = 1$ while in the second case $\text{sgn}(\vec{j}_i \times \vec{c}_i) = -1$. Since successive crossings, i and $i+1$, must occur in opposite directions:

$$\text{sgn}(\vec{j}_i \times \vec{c}_i) + \text{sgn}(\vec{j}_{i+1} \times \vec{c}_{i+1}) = 0$$

Since in the course of a complete circuit, C must intersect J an even number of times,

$$\sum_{i=0}^{m-1} \text{sgn}(\vec{j}_i \times \vec{c}_i) = \sum_{i=0}^{m/2-1} \text{sgn}(\vec{j}_{2i} \times \vec{c}_{2i}) + \text{sgn}(\vec{j}_{2i+1} \times \vec{c}_{2i+1}) = 0 \quad \square$$

We now proceed with the proof that the sums of the weights around every closed cycle in a network constructed as described equal zero. Assign locations in the plane to the vertices in the network, such that each vertex is located within its respective planar region. Since edges only connect vertices located in adjacent planar regions, the network clearly has a planar embedding. We further note that every edge in the network need only cross an edge in the labeled figure once: At the boundary between adjacent regions. Furthermore, at these crossing points, the signs of the cross products of vectors tangent to edges of the network and edges of the labeled figure are everywhere equal to 1, which equals half the network edge weight when traversed in the direction of its orientation. Conversely, if the edge is traversed in the opposite direction, then the sign of the cross product is -1, which again corresponds to half the weight of the network edge. It follows that when a simple cycle is traversed in a given direction, the signs of the cross products of vectors tangent to the cycle and the edges of the labeled figure equal one half the weights of the network edges. Since the network is a planar graph, the traversal of every simple cycle (i.e. a cycle in which no vertex is visited twice) traces an oriented Jordan curve in the plane. Therefore by the lemma just proved, the sum of the weights for simple cycles is zero. Complex cycles, in turn, are the sums of one or more simple cycles, each of which is an oriented Jordan curve. Clearly then, the sums of the weights around every cycle in the network also equals zero, so that the system of difference equations always has a solution.

Let us summarize the proof to this point. We began with the observation that a set of closed plane-curves partitions the plane into regions. We then described a system of difference equations which the multiplicities of the projection of interior surface points onto the different regions must satisfy if the plane-curves are occluding contours. It was subsequently shown that a solution to this system of difference equations can always be found.

The second part of the proof is a description of a procedure for constructing a paneling given a labeled figure and a solution to the system of difference equations. We then demonstrate that the neighborhood of every point of the paneling is homeomorphic to a disc, so that the paneling must represent a surface without boundary. Furthermore, the nature of the construction guarantees that the paper model can be assembled without self-intersection, so that the surface must also be orientable. Together, this establishes that the paneling represents the boundary of a manifold-solid.

2.1 Paneling Construction

Since each region of the planar partition induced by the labeled figure is a topological disc, flat panels of the same shape and size can be cut out from a sheet of paper. Let us further assume that the paper is white on one side and black on the other side. For each region, R, create γ_R copies of the paper panel, where γ_R is a solution to the above system of difference equations. Let the copies of region R be $R(1), R(2), ..., R(\gamma_R)$ and let them be arranged in a stack above region R in the plane such that $R(1)$ is the uppermost region and $R(\gamma_R)$ is the lowermost region. This is done so that the white side of each panel faces upward and the black side of each panel faces downward.

Let A and B be neighboring regions and let n be the depth index of the edge separating them. Note that if A lies to the right of B then $\gamma_A - \gamma_B = 2$. Unless n equals zero, identify the side (bordering B) of each panel (above region A) numbered 1 through n with the adjacent side of the corresponding copy of region B such that white is glued to white (i.e. $A(1) \rightleftharpoons B(1), ..., A(n) \rightleftharpoons B(n)$). Then identify the side of $A(n+1)$ (adjacent to B) with the side of $A(n+2)$ (also adjacent to B) such that white and black meet (i.e. $A(n+1) \Rightarrow A(n+2)$). We call an edge where white and black meet a *fold edge* (See Figure 9). Now, unless γ_A equals $n+2$, identify the side (bordering B) of each panel (above region A) numbered $n+3$ through γ_A with the adjacent side of the copy of region B numbered $n+1$ through $\gamma_A - 2$ such that white is glued to white (i.e. $A(n+3) \rightleftharpoons B(n+1), ..., A(\gamma_A) \rightleftharpoons B(\gamma_A - 2)$). We refer to this implicitly defined set of edge identifications as the *identification scheme.* The effect of the identification scheme is to create n interior edges above and $\gamma_A - n - 2$ interior edges beneath a fold edge in the paneling. The set of identifications can be divided into three subranges, the first and last of which are potentially empty:[2]

(a) $A(1) \rightleftharpoons B(1), ..., A(n) \rightleftharpoons B(n)$

(b) $A(n+1) \Rightarrow A(n+2)$

(c) $A(n+3) \rightleftharpoons B(n+1), ..., A(\gamma_A) \rightleftharpoons B(\gamma_A - 2)$

By everywhere gluing along the edges specified by the identification scheme, a paneling is created. However, we still must show that this paneling represents a manifold-solid. This will be done by demonstrating that the neighborhood of every point of the paneling has structure characteristic of an interior surface point (i.e. is homeomorphic to a disc). Towards this end, we observe that points of the paneling can be divided into the following categories: 1) Points interior to a panel; 2) Points lying on a panel edge; 3) Vertices originating in crossings; and 4) Vertices originating in cusps. In each of these cases, we demonstrate that the neighborhood of the point is homeomorphic to a disc.

The first two cases are trivial. First, it is clear that a point interior to a panel forms an interior point of the surface. Second, the nature of the identification scheme ensures that every panel edge is identified with one and only one other edge. Pairs of identified panel edges therefore form interior edges of the paneling. This leaves only the last two cases.

We therefore consider the neighborhood structure of paneling vertices. These are points where the corners of two or more panels meet and are created when the construction is applied to the edges incident to a crossing or cusp in the labeled figure. We note that the result need only be demonstrated for one of the two crossing labels and one of the two cusp labels since the other two are mirror images.

[2]If the final index of a subrange is less than the initial index, then that subrange is empty.

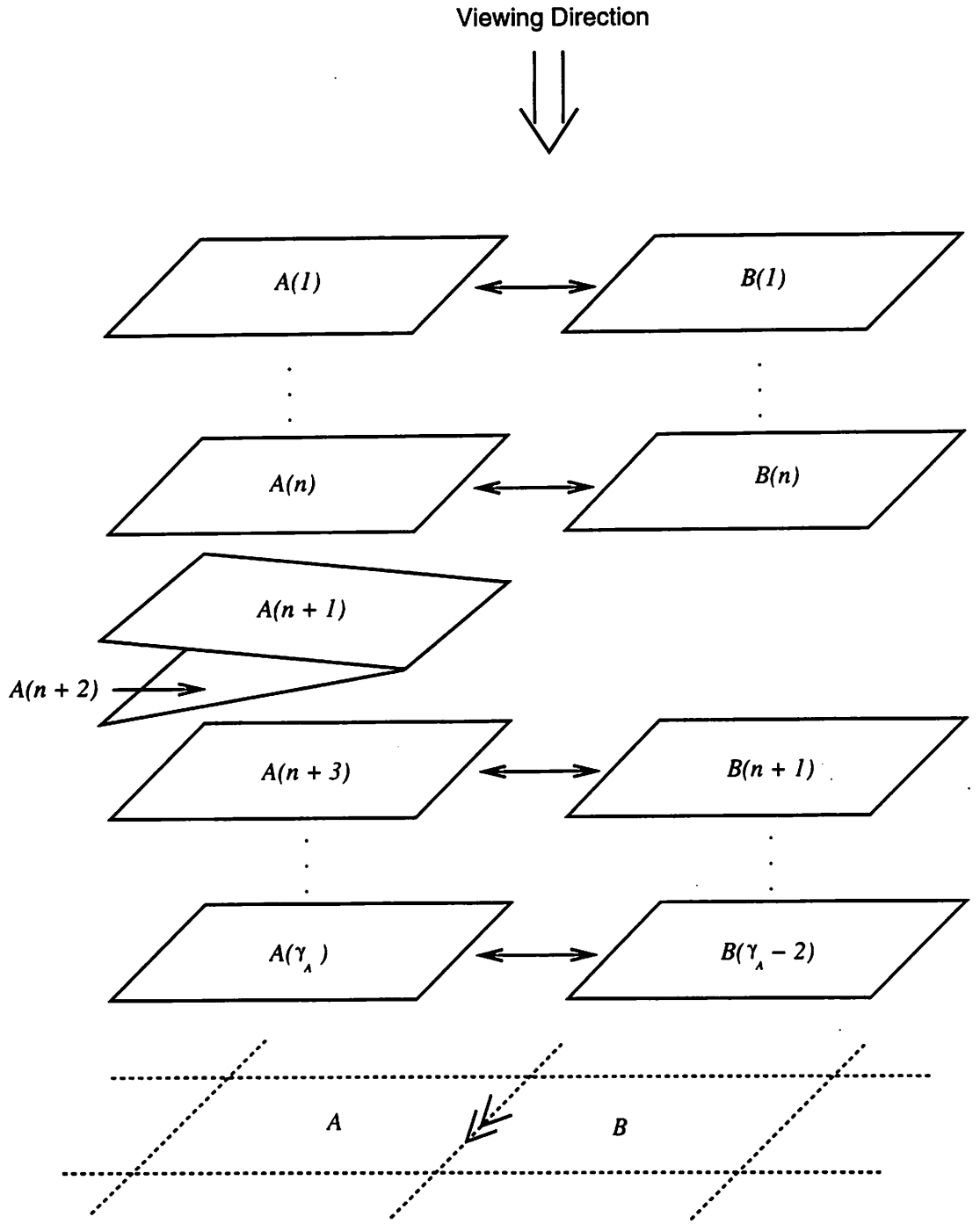

Figure 8: Paper panels stacked above region A and B in the plane. Following the *identification scheme*, all copies of regions A and B but $A(n+1)$ and $A(n+2)$ are glued along their adjacent sides. Copies $A(n+1)$ and $A(n+2)$ are glued to form a *fold edge*.

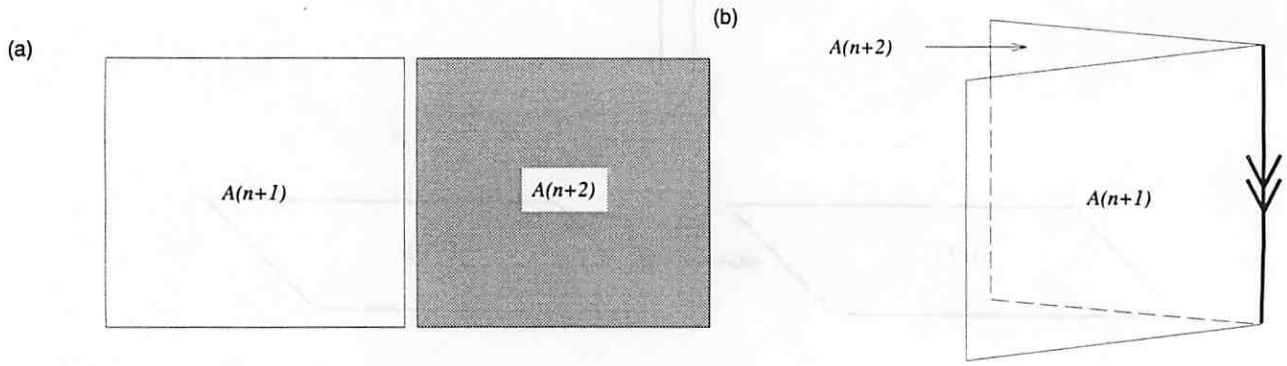

Figure 9: (a) Flattened view of $A(n+1) \Rightarrow A(n+2)$. (b) The *fold edge* which results.

2.2 Neighborhoods of Crossing Vertices

We treat the case of the crossing first. Let the four regions incident at a crossing with writhe equal to $+1$ be A, B, C and D as illustrated in Figure 10. Note that the depth index of the edges dividing regions A and B is m, regions C and D is m, regions A and C is $n+2$, and regions B and D is n, with $0 \leq m \leq n \leq \gamma_C$ as guaranteed by the labeling scheme. Since region C lies to the right of both occluding contours, the multiplicity of region C is two greater than the multiplicity of regions A and D (i.e. $\gamma_C = \gamma_D + 1 = \gamma_A + 2$) and four greater than the multiplicity of region B (i.e. $\gamma_C = \gamma_B + 4$). We will show that, after gluing, each of the γ_C copies of region C will form a vertex with a neighborhood homeomorphic to a disc. In the process, all copies of the other three regions will be accounted for.

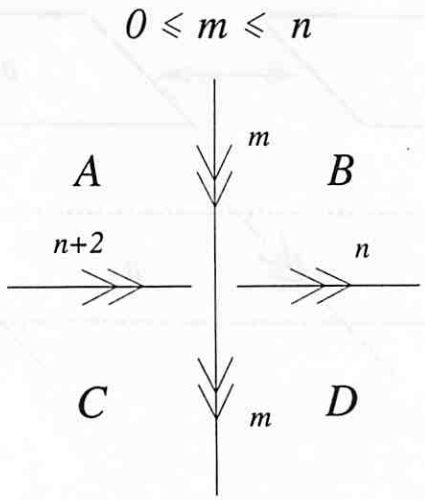

Figure 10: Four regions incident at a crossing with writhe equal to $+1$.

We begin by enumerating the set of edge identifications prescribed by the identification scheme for copies of regions A, B, C and D. These identifications are understood to apply to the adjacent edges of the specified copies:

1. Identifications between copies of A and B.

(a) $A(1) \rightleftharpoons B(1), ..., A(m) \rightleftharpoons B(m)$

(b) $A(m+1) \Rightarrow A(m+2)$

(c) $A(m+3) \rightleftharpoons B(m+1), ..., A(\gamma_A) \rightleftharpoons B(\gamma_A - 2)$

2. Identifications between copies of C and D.

(a) $C(1) \rightleftharpoons D(1), ..., C(m) \rightleftharpoons D(m)$

(b) $C(m+1) \Rightarrow C(m+2)$

(c) $C(m+3) \rightleftharpoons D(m+1), ..., C(\gamma_C) \rightleftharpoons D(\gamma_C - 2)$

3. Identifications between copies of C and A.

(a) $C(1) \rightleftharpoons A(1), ..., C(n+2) \rightleftharpoons A(n+2)$

(b) $C(n+3) \Rightarrow C(n+4)$

(c) $C(n+5) \rightleftharpoons A(n+3), ..., C(\gamma_C) \rightleftharpoons A(\gamma_C - 2)$

4. Identifications between copies of D and B.

(a) $D(1) \rightleftharpoons B(1), ..., D(n) \rightleftharpoons B(n)$

(b) $D(n+1) \Rightarrow D(n+2)$

(c) $D(n+3) \rightleftharpoons B(n+1), ..., D(\gamma_D) \rightleftharpoons B(\gamma_D - 2)$

The identifications can be grouped into five consecutive subranges instead of three by exploiting the fact that $\gamma_C = \gamma_A + 2 = \gamma_D + 2 = \gamma_B + 4$ and $0 \leq m \leq n \leq \gamma_C$:

1. Identifications between copies of A and B.

(a) $A(1) \rightleftharpoons B(1), ..., A(m) \rightleftharpoons B(m)$

(b) $A(m+1) \Rightarrow A(m+2)$

(c) $A(m+3) \rightleftharpoons B(m+1), ..., A(n+2) \rightleftharpoons B(n)$

(d) None.

(e) $A(n+3) \rightleftharpoons B(n+1), ..., A(\gamma_C - 2) \rightleftharpoons B(\gamma_C - 4)$

2. Identifications between copies of C and D.

(a) $C(1) \rightleftharpoons D(1), ..., C(m) \rightleftharpoons D(m)$

(b) $C(m+1) \Rightarrow C(m+2)$

(c) $C(m+3) \rightleftharpoons D(m+1), ..., C(n+2) \rightleftharpoons D(n)$

(d) $C(n+3) \rightleftharpoons D(n+1), C(n+4) \rightleftharpoons D(n+2)$

(e) $C(n+5) \rightleftharpoons D(n+3), ..., C(\gamma_C) \rightleftharpoons D(\gamma_C - 2)$

3. Identifications between copies of C and A.

(a) $C(1) \rightleftharpoons A(1), ..., C(m) \rightleftharpoons A(m)$

(b) $C(m+1) \rightleftharpoons A(m+1), C(m+2) \rightleftharpoons A(m+2)$

(c) $C(m+3) \rightleftharpoons A(m+3), ..., C(n+2) \rightleftharpoons A(n+2)$

(d) $C(n+3) \Rightarrow C(n+4)$

(e) $C(n+5) \rightleftharpoons A(n+3), ..., C(\gamma_C) \rightleftharpoons A(\gamma_C - 2)$

4. Identifications between copies of D and B.

(a) $D(1) \rightleftharpoons B(1), ..., D(m) \rightleftharpoons B(m)$

(b) None.

(c) $D(m+1) \rightleftharpoons B(m+1), ..., D(n) \rightleftharpoons B(n)$

(d) $D(n+1) \Rightarrow D(n+2)$

(e) $D(n+3) \rightleftharpoons B(n+1), ..., D(\gamma_C - 2) \rightleftharpoons B(\gamma_C - 4)$

The effect of gluing the panels according to the prescribed identifications is best illustrated by means of a diagram such as Figure 11. Pairs of identified edges are adjacent in the diagram. This diagram illustrates, in the most general case, the vertices of the paneling which are produced by the construction when applied at a single crossing. The fact that these and only these vertices are created can be verified by noting that: 1) Every identification prescribed by the identification scheme appears in the diagram; and 2) Every identification appearing in the diagram is prescribed by the identification scheme.

The effect of identifications 1-4 (b) and (d) is to create two fold edges. The effect of identifications 1-4 (a),(c) and (e) is: 1) To create m interior vertices above the upper fold edge. 2) To create $n - m$ interior vertices between the upper and lower fold edges; and 3) To create $\gamma_C - n - 4$ interior vertices beneath the lower fold edge. Clearly, if $m = 0$ then no interior vertices are created above the upper fold edge. Similiarly, if $m = n$ then no interior vertices are created between the upper and lower fold edge. Finally, if $n = \gamma_c - 4$, no interior vertices are created beneath the lower fold edge. Inspection of the diagram confirms that exactly four panels meet at each vertex, and that the neighborhood of each vertex is homeomorphic to a disc.

2.3 Neighborhoods of Cusp Vertices

We now show that the neighborhoods of all paneling vertices created when the construction is applied to the edges incident at a cusp are also homeomorphic to discs. Let the two regions adjacent to the cusp be A and B as illustrated in Figure 12. Note that two different edges of the labeled figure (i.e. the *near* and *far* edges) separate region A from region B. The depth index of the near edge is n and the depth index of the far edge is $n+1$. Since region A lies to the right of both edges, the multiplicity of region A is two greater than the multiplicity of region B (i.e. $\gamma_A = \gamma_B + 2$). We will show that, after gluing, each of the γ_A copies of region A will form a vertex with a neighborhood homeomorphic to a disc. In the process, all copies of region B will be accounted for.

We begin by enumerating the set of identifications prescribed by the identification scheme for each edge:

1. Identifications between A and B across near edge.

(a) $A(1) \rightleftharpoons B(1), ..., A(n) \rightleftharpoons B(n)$

(b) $A(n+1) \Rightarrow A(n+2)$

(c) $A(n+3) \rightleftharpoons B(n+1), ..., A(\gamma_A) \rightleftharpoons B(\gamma_A - 2)$

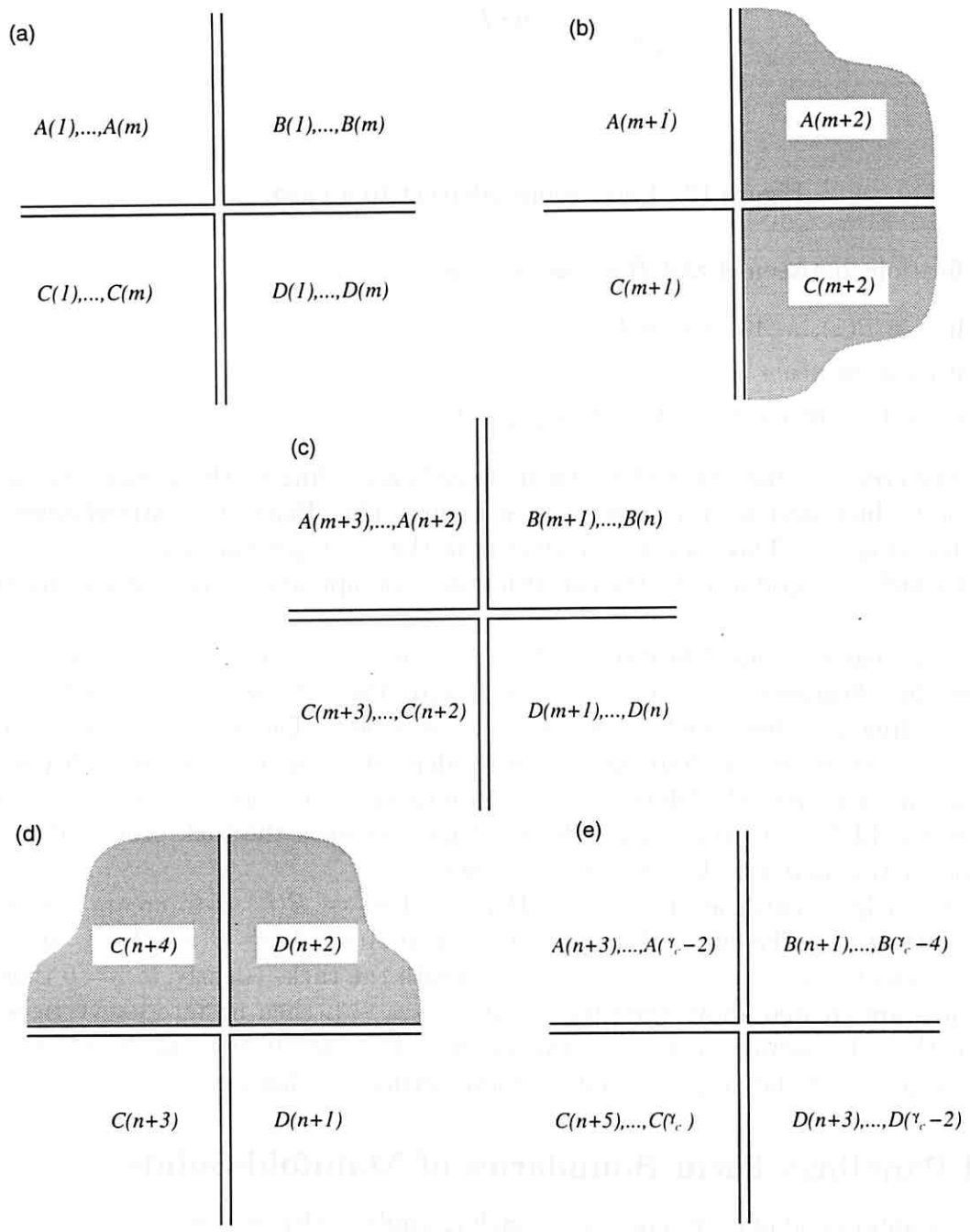

Figure 11: Paneling vertices produced by the construction when applied to edges incident at a crossing.

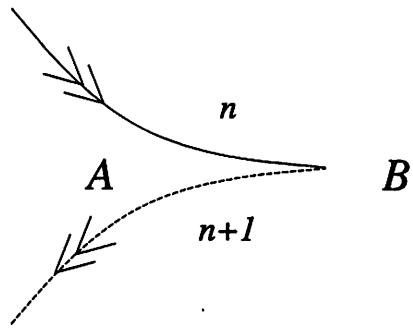

Figure 12: Two regions adjacent to a cusp.

2. Identifications between A and B across far edge.

   (a) $A(1) \rightleftharpoons B(1), ..., A(n+1) \rightleftharpoons B(n+1)$

   (b) $A(n+2) \Rightarrow A(n+3)$

   (c) $A(n+4) \rightleftharpoons B(n+2), ..., A(\gamma_A) \rightleftharpoons B(\gamma_A - 2)$

As with the crossing, the effect of gluing the panels according to the prescribed identifications is best illustrated with a diagram (See Figure 13). Pairs of identified edges are adjacent in the diagram. This diagram illustrates, in the most general case, the vertices of the paneling which are produced by the construction when applied to the edges incident at a cusp.

The effect of near edge identifications $A(n+1) \Rightarrow A(n+2)$ and $A(n+3) \rightleftharpoons B(n+1)$, and far edge identifications $A(n+1) \rightleftharpoons B(n+1)$ and $A(n+2) \Rightarrow A(n+3)$ is to create a folded embedding of a disc which we will refer to as a *tuck*. The unfolded disc is shown in Figure 13(d). Observe that four panels are incident at a single paneling vertex which is homeomorphic to a disc. By folding the disc as illustrated in Figure 13(e), the tuck is created. Figures 13(f) and (g) illustrate the similiarity between the tuck produced by the paneling construction and a tuck in a smooth surface.

The effect of edge identifications $A(1) \rightleftharpoons B(1), ..., A(n) \rightleftharpoons B(n)$ is to create n interior vertices above the tuck. The effect of edge identifications $A(n+4) \rightleftharpoons B(n+2), ..., A(\gamma_A) \rightleftharpoons B(\gamma_A - 2)$ is to create $\gamma_A - n - 4$ interior vertices beneath the tuck. Clearly, if $n = 0$ then no interior vertices are created above the tuck and if $n = \gamma_A - 4$, then no interior vertices are created beneath it. Inspection of the diagram confirms that exactly two panels are incident at each vertex, and that the neighborhoods of these vertices are homeomorphic to discs.

2.4 All Panelings Form Boundaries of Manifold-Solids

Because the neighborhood of every point of a paneling produced by the construction is homeomorphic to a disc, it follows that all such panelings represent surfaces without boundary. Furthermore, because the construction guarantees that the panelings can be embedded in three-dimensional space without self-intersection, the surfaces without boundary must be orientable. We therefore conclude that all panelings generated by the construction represent the boundaries of manifold-solids.

We now show that the image of the surface without boundary produced by the construction corresponds to the labeled figure in every respect and that the view is generic. First,

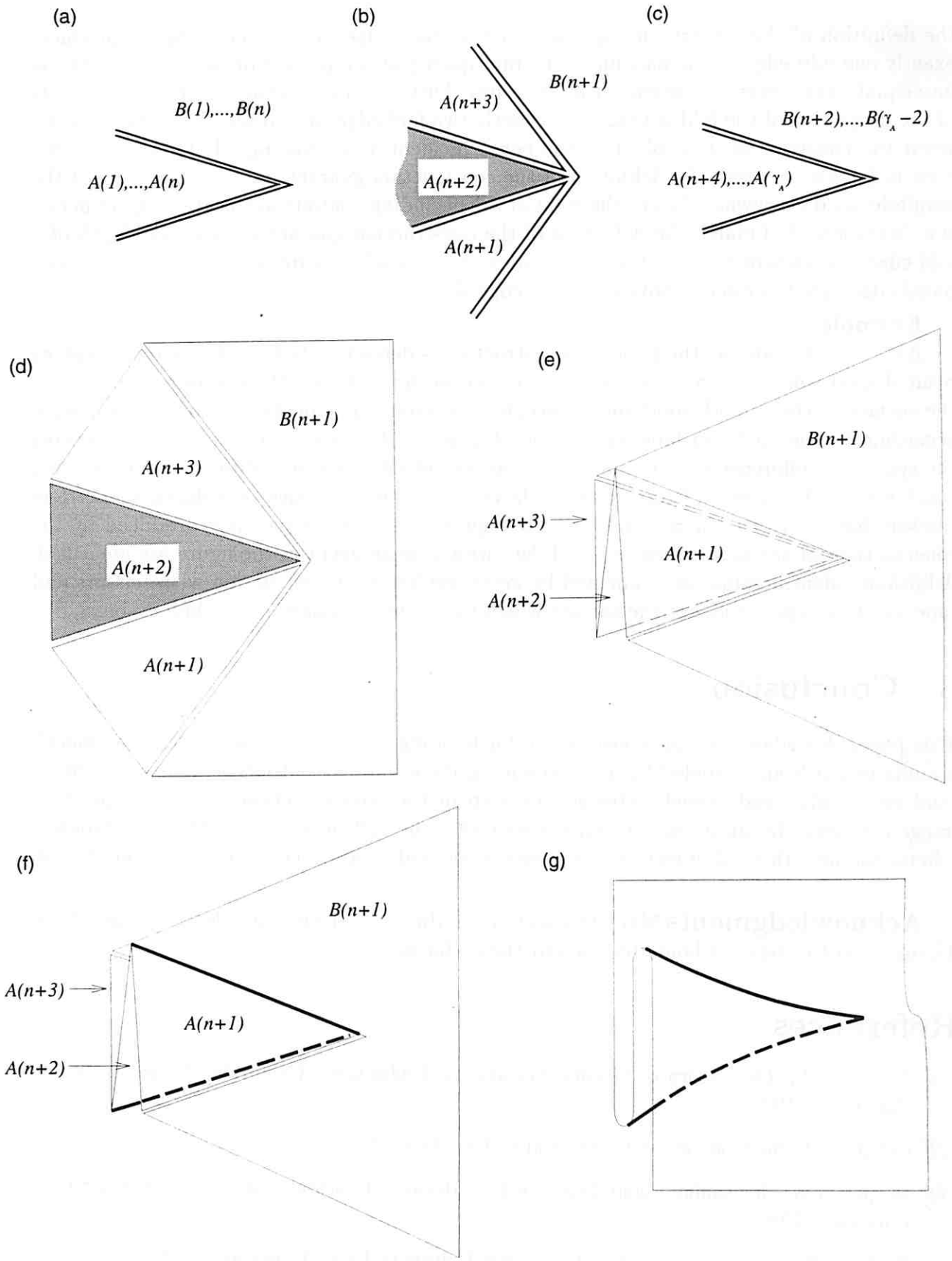

Figure 13: (a-c) Paneling vertices produced by the construction when applied to edges incident at a cusp. (d) Unfolded disc. (e) Folded embedding of disc. (f) Same as (e) but with occluding contour superimposed. (g) Tuck in a smooth surface.

the definition of the construction guarantees that each edge in the labeled figure produces exactly one fold edge in the paneling. The multiplicity of the projection of the fold is therefore equal to one everywhere except at crossings. Furthermore, at crossings the multiplicity of the projection of the fold is two, since exactly two fold edges are produced in the paneling when the construction is applied to the edges incident at a crossing. It follows that the view is generic. Second, the definition of the construction guarantees that the image of the manifold-solid everywhere lies to the right of the occluding contour so that the sign of occlusion is respected. Finally, the definition of the construction guarantees that the depth of a fold edge everywhere matches the depth index of the labeled figure, since exactly n interior panel edges are assembled above each fold edge.□

Example

As a simple example, the paneling construction is demonstrated for the case of a kidney bean shaped solid. Figure 14(a) shows the relationship between the contour generator on the surface of the smooth solid and its occluding contour. The occluding contour is labeled according to the Huffman labeling scheme. Figure 14(b) shows the network representing the system of difference constraints which must be solved as a precondition for the paneling construction. The labeled figure is shown dashed while network edges are shown solid. Here the solution is $\gamma_A = 4$, $\gamma_B = 2$ and $\gamma_C = 0$. Figure 15 shows the paneling produced by the construction for the kidney bean solid. Edges which are adjacent in the figure are identified. Additional identifications are indicated by lowercase letters. Construction with scissors and tape yields a paper model of the surface which forms the boundary of the kidney bean.

3 Conclusion

This paper describes a simple construction for building a combinatorial model of a smooth manifold-solid from a labeled figure representing its occluding contour. This is an essential (and previously unaddressed) intermediate step in the reconstruction of solid-shape from image contours. In addition, this paper establishes the sufficiency of the Huffman labeling scheme for smooth solid-objects as a representation and as a source of grouping constraints.

Acknowledgments Many thanks to Ivan Mirkovic for his valuable insight and help. Thanks also to Chakra Chennubhotla and David Jacobs.

References

[1] Arnold, V.I., *The Theory of Singularities and its Applications*, Cambridge University Press, Cambridge, 1991.

[2] Callahan, J., Singularities and plane maps, *Am. Math. Monthly 81*, 1974.

[3] Draper, S.W., Reasoning about Depth in Line-Drawing Interpretation, Ph.D. thesis, Sussex University, 1980.

[4] Griffiths, H.B., *Surfaces*, 2nd Ed., Cambridge University Press, Cambridge, 1981.

[5] Henle, M., *A Combinatorial Introduction to Topology*, W.H. Freeman and Co., San Francisco, Cal., 1979.

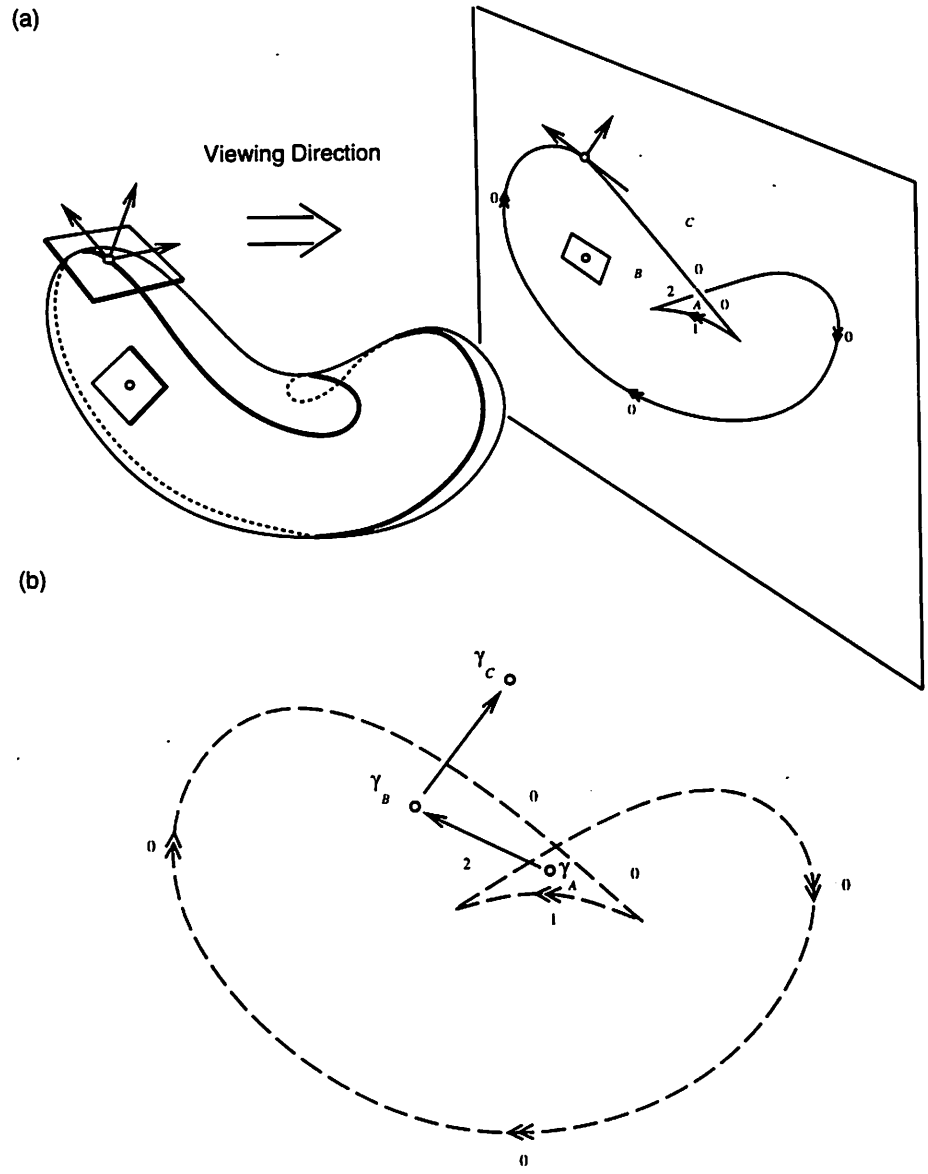

Figure 14: (a) A kidney bean shaped solid. The *contour generator* is the locus of surface points tangent to the viewing direction (i.e. the pre-image of the occluding contour). Cusps occur where the contour generator is asymptotic to the viewing direction. Here the occluding contour contains two cusps which form a "swallowtail." [Note: This figure is adapted from a figure by Jim Callahan[2].] (b) The network representing the system of difference equations which must be solved as a precondition for the paneling construction. The labeled figure is shown dashed while network edges are shown solid. Here the solution is $\gamma_A = 4$, $\gamma_B = 2$ and $\gamma_C = 0$.

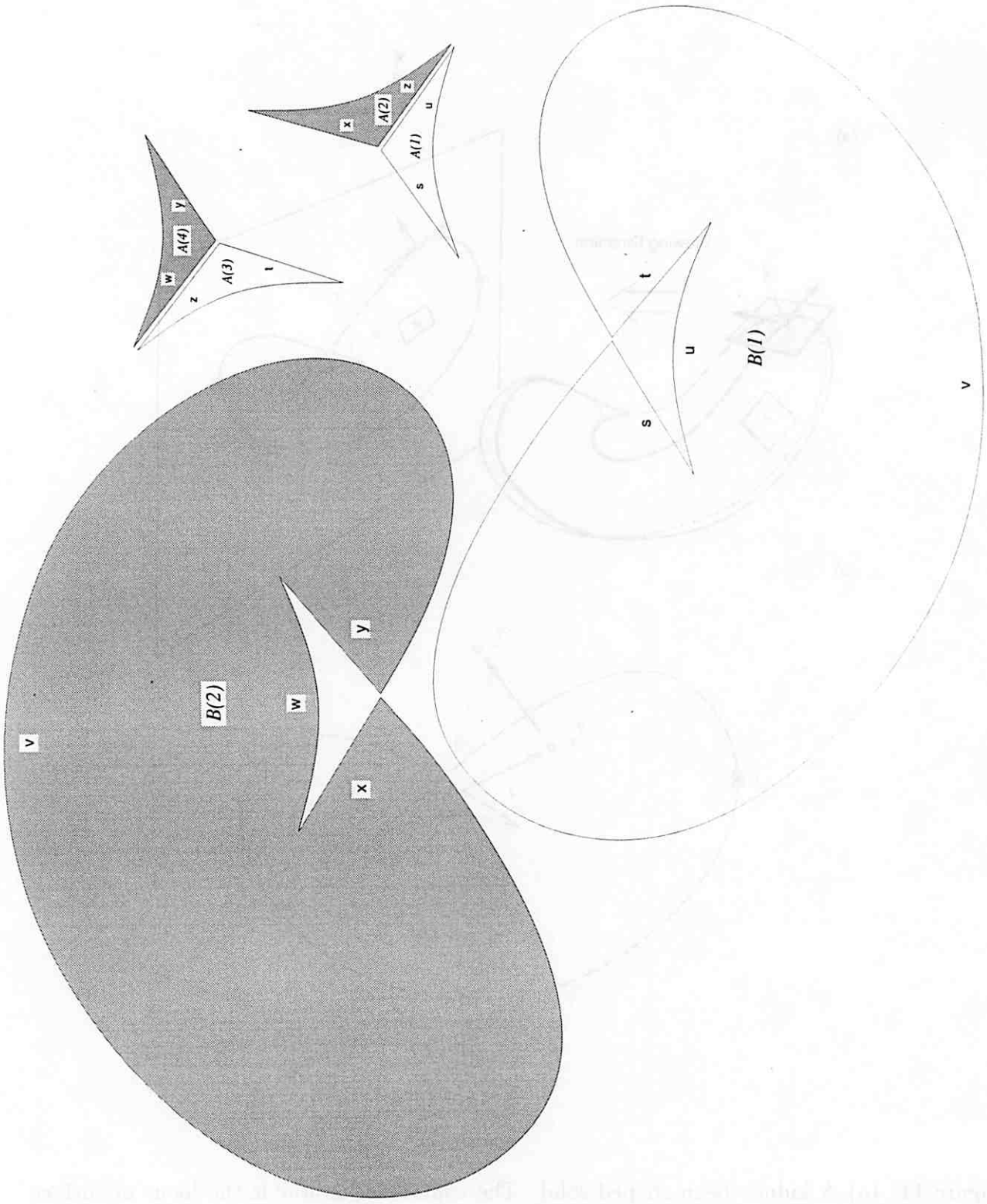

Figure 15: Paneling produced by the construction for the kidney bean solid. Edges which are adjacent are identified. Additional identifications are indicated by lowercase letters. Construction with scissors and tape yields a paper model of the surface which forms the boundary of the kidney bean.

[6] Huffman, D.A., Impossible Objects as Nonsense Sentences, *Machine Intelligence 6*, B. Meltzer and D. Michie (eds.), American Elsevier Publishing Co., New York, 1971.

[7] Kanade, T., Recovery of the Three-dimensional Shape of an Object from a Single View, *Artificial Intelligence 17*, pp. 409-460, 1981.

[8] Kanizsa, G., *Organization in Vision*, Praeger, New York, 1979.

[9] Koenderink, J.J., and A.J. van Doorn, The singularities of the visual mapping, *Biological Cybernetics 24*, 1976.

[10] Malik, J., Interpreting Line Drawings of Curved Objects, *Intl. Journal of Computer Vision*, Vol. 1, No. 1, pp. 73-103, 1987.

[11] Paul, G.S., *Predatory Dinosaurs of the World: A Complete Illustrated Guide*, Simon and Schuster, New York, 1988.

[12] Richards, W. and Koenderink J.J., and D.D. Huffman, Inferring 3D Shapes from 2D Silhouettes, *Natural Computation*, W. Richards (ed.), MIT Press, Cambridge, Mass., 1988.

[13] Seifert, H. and Threlfall, *A Textbook of Topology*, Academic Press, Boston, Mass., 1980.

[14] Szeliski, R. and Tonnesen, D., and D. Terzopolous, Modeling Surfaces of Arbitrary Topology with Dynamic Particles, *IEEE Conference on Computer Vision and Pattern Recognition*, New York City, June 1993.

[15] Terzopolous, D., Witkin, A. and M. Kass, Symmetry-Seeking Models for 3D Object Reconstruction, *Proc. of the 1st Intl. Conf. on Computer Vision*, London, England, 1987.

[16] Waltz, D., Understanding Line Drawings of Scenes with Shadows, *Psychology of Computer Vision*, P.H. Winston (ed.), McGraw Hill, New York, 1975.

[17] Whitney, H., On singularities of mappings of Euclidean spaces I: Mappings of the plane into the plane, *Ann. of Math. 62*, 1955.

[18] Williams, L.R., Perceptual Organization of Occluding Contours, *Proc. of the 3rd Intl. Conf. on Computer Vision*, Osaka, Japan, 1990.

[19] Williams, L.R., Perceptual Completion of Occluded Surfaces, Ph.D. dissertation, Dept. of Computer Science, University of Massachusetts, Amherst, Mass., 1994.